European Journal of Nuclear Medicine and Molecular Imaging (2021) 48:414–420
https://doi.org/10.1007/s00259-020-04878-9

ORIGINAL ARTICLE

In vivo quantitative mapping of human mitochondrial cardiac membrane potential: a feasibility study

Matthieu Pelletier-Galarneau[1] · Yoann Petibon[1] · Chao Ma[1] · Paul Han[1] · Sally Ji Who Kim[1] · Felicitas J. Detmer[1] · Daniel Yokell[1] · Nicolas Guehl[1] · Marc Normandin[1] · Georges El Fakhri[1] · Nathaniel M. Alpert[1]

Received: 13 March 2020 / Accepted: 19 May 2020 / Published online: 27 July 2020

Abstract

Purpose Alteration in mitochondrial membrane potential ($\Delta\Psi_m$) is an important feature of many pathologic processes, including heart failure, cardiotoxicity, ventricular arrhythmia, and myocardial hypertrophy. We present the first in vivo, non-invasive, assessment of regional $\Delta\Psi_m$ in the myocardium of normal human subjects.

Methods Thirteen healthy subjects were imaged using [^{18}F]-triphenylphosphonium ([^{18}F]TPP+) on a PET/MR scanner. The imaging protocol consisted of a bolus injection of 300 MBq followed by a 120-min infusion of 0.6 MBq/min. A 60 min, dynamic PET acquisition was started 1 h after bolus injection. The extracellular space fraction (f_{ECS}) was simultaneously measured using MR T1-mapping images acquired at baseline and 15 min after gadolinium injection with correction for the subject's hematocrit level. Serial venous blood samples were obtained to calculate the plasma tracer concentration. The tissue membrane potential ($\Delta\Psi_T$), a proxy of $\Delta\Psi_m$, was calculated from the myocardial tracer concentration at secular equilibrium, blood concentration, and fECS measurements using a model based on the Nernst equation.

Results In 13 healthy subjects, average tissue membrane potential ($\Delta\Psi_T$), representing the sum of cellular membrane potential ($\Delta\Psi_c$) and $\Delta\Psi_m$, was − 160.7 ± 3.7 mV, in excellent agreement with previous in vitro assessment.

Conclusion In vivo quantification of the mitochondrial function has the potential to provide new diagnostic and prognostic information for several cardiac diseases as well as allowing therapy monitoring. This feasibility study lays the foundation for further investigations to assess these potential roles.

Clinical trial identifier: NCT03265431

Keywords Positron emission tomography · Mitochondrial membrane potential · Tissue membrane potential · Triphenylphosphonium · Mitochondria

Introduction

Myocardial mitochondrial dysfunction plays a key role in many pathologic processes, including heart failure [1], cardiotoxicity [2], ventricular arrhythmia [3], and reperfusion injury [4]. Alteration in mitochondrial membrane potential ($\Delta\Psi_m$) is a fundamental biomarker of mitochondrial and cellular dysfunction as under normal conditions, $\Delta\Psi_m$ is maintained within narrow limits [5, 6]. Currently, there is no technique enabling non-invasive measurement of $\Delta\Psi_m$. In vitro measurements of $\Delta\Psi_m$ have been performed and validated for decades using fluorescent and radiolabeled lipophilic cation probes, including ^{3}H-tetraphenylphosphonium (^{3}H-TPP$^+$) [7–9]. The in vitro assays rely on long-lived β emitters and are thus inappropriate for human in vivo investigations. Our group recently described the first successful method for in vivo mapping of the tissue membrane potential, $\Delta\Psi_T$, a proxy of $\Delta\Psi_m$, in pigs, using the fluorinated compound [^{18}F]TPP$^+$ [10]. Using PET/CT imaging, we were able to map the left ventricular $\Delta\Psi_T$ in absolute units of millivolts

This article is part of the Topical Collection on Cardiology

Georges El Fakhri and Nathaniel M. Alpert are the co-last authors

✉ Georges El Fakhri
ELFAKHRI.GEORGES@mgh.harvard.edu

✉ Nathaniel M. Alpert
alpert@pet.mgh.harvard.edu

[1] Department of Radiology, Gordon Center for Medical Imaging, Massachusetts General Hospital, Harvard Medical School, 125 Nashua Street, #6604, Boston, MA 02114, USA

(mV). The obtained results were consistent with previous in vitro bench-top methods and confirmed the basic feasibility of quantitative in vivo mapping of $\Delta\Psi_T$. Here, we extend this method to healthy volunteers and describe the first in vivo imaging of $\Delta\Psi_T$ in humans.

Materials and methods

Patient population

Thirteen healthy subjects, 7 females and 6 males, aged between 41 and 74 years, without conditions or medication known to affect cellular membrane potential, such as diabetes, were studied. The study was conducted under the approval of the Partners Human Research Committee, the Institutional Review Board of Partners HealthCare.

Quantification of membrane potential

The method for in vivo quantification of $\Delta\Psi_T$ has been described in detail previously [10]. Briefly, we divide the tissue distribution space of [^{18}F]TPP$^+$ into three compartments: the extracellular space comprised of the interstitial and plasma space, the cytosol, and the mitochondria. Total activity in a voxel can be expressed as the sum of the activity in each compartment contained within that voxel. Therefore, at steady state, the concentration of [^{18}F]TPP$^+$ measured by PET in a voxel can be written as:

$$\overline{C}_{PET} = (1-f_{ECS})\left(f_{mito}\cdot\overline{C}_{mito} + (1-f_{mito})\cdot\overline{C}_{cyto}\right) + f_{ECS}\cdot\overline{C}_{ECS} \quad (1)$$

where $\overline{C}_{mito}$, $\overline{C}_{cyto}$, and $\overline{C}_{ECS}$, represent the steady-state concentration of [^{18}F]TPP$^+$ in the mitochondria, cytosol, and extracellular space respectively; f_{ECS} and f_{mito} represent the extracellular space fraction and mitochondrial fraction respectively. At equilibrium, the Nernst equation can be used to relate the concentration of tracer on each side of a membrane to its electric potential $\Delta\Psi$:

$$\frac{\overline{C}_{in}}{\overline{C}_{out}} = e^{-\beta\Delta\Psi} \quad (2)$$

where $\beta = \frac{zF}{RT}$ is the ratio of known physical parameters: z is the valence, F denotes Faraday's constant, R is the universal gas constant, and T is the temperature in degrees Kelvin. Noting that $\overline{C}_{ECS} = \overline{C}_p$ at steady state, division of Eq. 1 by $\overline{C}_p$ yields the following expression:

$$V_T = \frac{\overline{C}_{PET}}{\overline{C}_p} = (1-f_{ECS})\left(f_{mito}\cdot e^{-\beta(\Delta\Psi_m+\Delta\Psi_c)} + (1-f_{mito})\cdot e^{-\beta\Delta\Psi_c}\right) + f_{ECS} \quad (3)$$

where V_T, $\Delta\Psi_m$, and $\Delta\Psi_c$ represent the volume of distribution of the tracer, and the mitochondrial and cellular membrane potential respectively. Because V_T is >> 1, Eq. 3 can be approximated by

$$V_T \approx (1-f_{ECS})\cdot f_{mito}\cdot e^{-\beta(\Delta\Psi_T)} \quad (4)$$

where $\Delta\Psi_T$ is the total tissue membrane potential, defined as $\Delta\Psi_m + \Delta\Psi_c$. The f_{mito} parameter was assumed to be constant at 0.25 [11].

[^{18}F]*TPP*$^+$ synthesis

[^{18}F]TPP$^+$ was synthesized and purified on a GE Tracerlab FXN synthesis unit using [^{18}F]fluoride produced onsite by a GE PETtrace cyclotron bombarding > 98% enriched ^{18}O-water. The [^{18}F]TPP$^+$ was sterile filtered into a sterile vial and tested to ensure it met all FDA and USP specifications for a PET sterile radiopharmaceutical prior to injection. The radiation dose exposure from [^{18}F]TPP$^+$ is estimated at 0.0178 mSv/MBq, corresponding to an effective dose of 6.6 mSv for a dose of 370 mBq. [12]

PET/MR imaging

A bolus of 300 MBq of [^{18}F]TPP$^+$ was injected intravenously using PTFE tubing, immediately followed by an infusion of 0.6 MBq/min over 2 h, so that the magnitude of the bolus (K_{bol}) corresponds to 500 min of infusate. This bolus with infusion protocol allows the system to reach secular tracer equilibrium in the myocardium and blood. Approximately 60 min after the bolus injection, a 60-min PET acquisition in list mode was performed centered on the thorax. During PET acquisition, MR sequences were acquired before and after administration of gadolinium (Dotarem 0.5 mM/mL, 0.1 mM/kg) to measure the myocardium extracellular space fraction. Modified Look-Locker Inversion recovery (MOLLI) sequences were used to acquire T1 maps before and 15 min after contrast administration [13]. Dynamic PET images were reconstructed using an iterative algorithm (OSEM 3 iterations, 21 subsets) with 344 × 344 × 127 pixels and 1 min frame length. Attenuation correction was performed using a

segmentation method based on Dixon sequence with model-based bone estimation [14].

Extracellular space fraction quantification

Region-of-interests (ROIs) were drawn over the myocardium and left ventricular cavity on T1 images. The extracellular space (ECS) fraction was calculated using the following formula:

$$f_{ECS} = \frac{\left(\frac{1}{T_{1\ myo,post}} - \frac{1}{T_{1\ myo,pre}}\right)}{\left(\frac{1}{T_{1\ blood,post}} - \frac{1}{T_{1\ blood,pre}}\right)} \times (100 - Hct)\ . \qquad (5)$$

where $T_{1\ myo,\ pre}$ and $T_{1\ myo,\ post}$ each denote the T_1 of myocardium measured before and after gadolinium (Gd) injection, respectively; $T_{1\ blood,\ pre}$ and $T_{1\ blood,\ post}$ each denote the T_1 of blood measured before and after Gd injection, respectively; and *Hct* denotes hematocrit in percentage measured from blood samples.

Results

Characteristics of the studied population are presented in Table 1. For all 13 subjects, secular equilibrium was achieved after ≤ 90 min with relatively constant myocardial and blood tracer concentrations (Fig. 1b). For one subject, motion introduced significant artifacts in the PET images and only the motion-free portion of the acquisition was used for the analysis. Overall, the average f_{ECS} was 0.293 ± 0.025 and ranged from 0.261 to 0.339. Average V_T was 73.3 ± 12.0 and ranged from 60.4 to 106.7. Average $\Delta\Psi_T$ was − 160.7 ± 3.7 mV and ranged from − 170.4 to − 156.2 mV (Fig. 1c). Values of $\Delta\Psi_T$ across the standard 17 left ventricular segments were homogeneous (Fig. 1d, Table 2).

With this method, high-quality parametric images of $\Delta\Psi_T$ can be generated, allowing for regional assessment of $\Delta\Psi_T$ (Fig. 2). In our sample, no significant correlations between age and f_{ECS} ($R^2 = 0.06579$, $p = 0.40$) or between age and $\Delta\Psi_T$ ($R^2 = 0.0340$, $p = 0.55$) were observed (Fig. 3). In addition, there was no significant difference between male and female in f_{ECS} (0.284 ± 0.025 vs 0.301 ± 0.024, $p = 0.23$) and $\Delta\Psi_T$ (− 162.4 ± 4.4 vs − 159.2 ± 2.2 mV, $p = 0.11$).

Table 1 Population characteristics

Female, *N* (%)	7 (53.8%)
Age (year), mean ± SD (range)	56 ± 10 (41–74)
Ethnicity, *N* (%)	
Caucasian	11 (84.6%)
African American	1 (7.7%)
Hispanic	0 (0.0%)
Asian	1 (7.7%)
BMI (kg/m^2), mean ± SD (range)	25.4 ± 3.5 (18.8–31.5)
Hypertension, *N* (%)	
No	11 (84.6%)
Yes	2 (15.4%)
Diabetes, *N* (%)	
No	13 (100.0%)
Yes	0 (0.0%)
Smoking, *N* (%)	
Never	12 (92.3%)
Current	0 (0.0%)
Remote (> 1 year)	1 (7.7%)
Dyslipidemia, *N* (%)	
No	13 (100.0%)
Yes	0 (0.0%)
Heart rate (min^{-1})	66 ± 14 (46–96)
Systolic blood pressure (mmHg)	127 ± 20 (101–173)
Diastolic blood pressure (mmHg)	78 ± 7 (64–87)
Rate pressure product (mmHg/min)	8297 ± 1949 (5757–12,032)

Discussion

Quantification of $\Delta\Psi_m$ has been performed in vitro by measuring the concentration of different lipophilic cations in mitochondria. These molecules cross the cellular and mitochondrial phospholipid membranes without significant interaction, and their concentration on either side of a membrane at equilibrium abide by the Nernst equation. In this study, we demonstrated for the first time the feasibility of in vivo quantification of $\Delta\Psi_T$, a proxy of $\Delta\Psi_m$, in humans. The method presented in this work relies on the exact same principle on which in vitro techniques are founded but uses PET imaging to measure tissue concentration of the lipophilic cation [^{18}F]TPP$^+$. The total tissue membrane potential, $\Delta\Psi_T$, is often used instead of $\Delta\Psi_m$ for in vitro studies, including explanted hearts, as isolation of the different cellular compartment is not easily feasible [9, 15].

As normal mitochondrial function depends on the maintenance of membrane potential in a narrow range, pathologies associated with mitochondrial dysfunction could potentially be studied with membrane potential tracers such as [^{18}F]TPP$^+$. Indeed, several pathologies have been associated with mitochondrial dysfunction, including cancers [16], diabetes [17], and cardiotoxicity [18]. The first attempt to measure $\Delta\Psi_T$ in vivo has been reported over 30 years ago by Fukuda et al. [15] who studied the distribution of the lipophilic cation triphenylmethylphosphonium labeled with ^{11}C (^{11}C-TPMP) [15]. Using primitive PET systems, they reported $\Delta\Psi_T$ in dogs (− 148.1 ± 6.0 mV), rats (− 146.7 ± 3.8 mV),

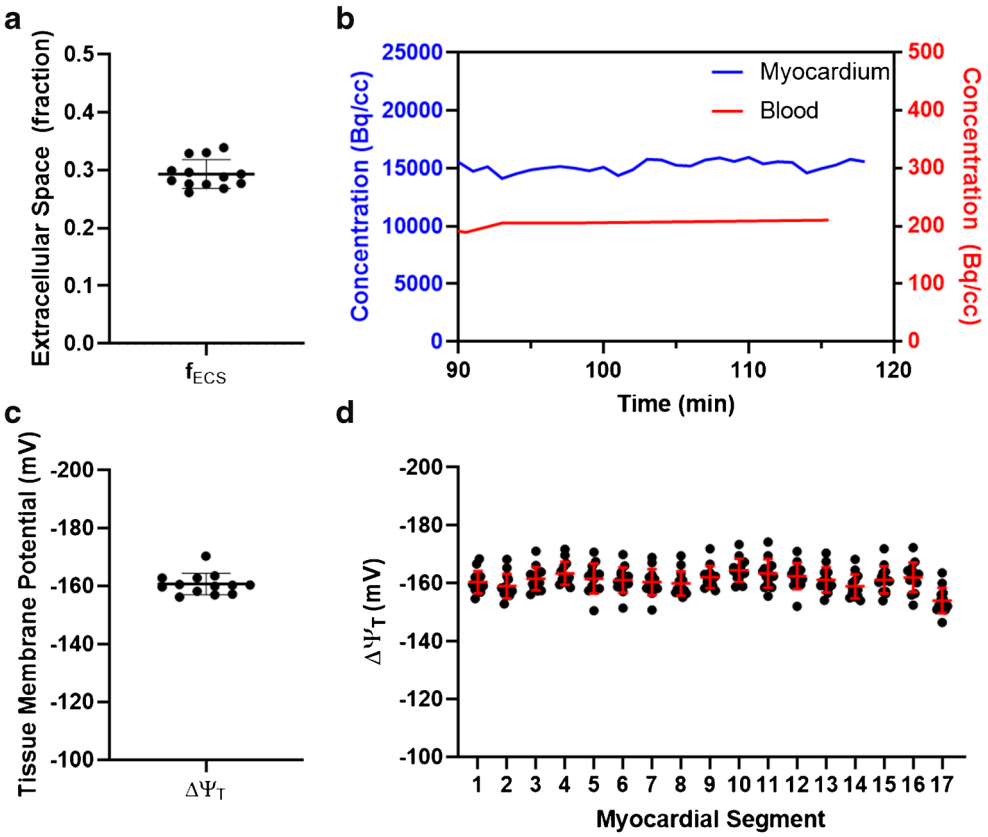

Fig. 1 **a** Average extracellular fraction (f_{ECS}) of the 13 study subjects. **b** Time activity curves (TAC) of a representative subject showing that tracer concentrations in the blood and in the myocardium are at secular equilibrium between 90 and 120 min post tracer injection. **c** Average tissue membrane potential ($\Delta\Psi_T$) of the 13 study subjects. D, $\Delta\Psi_T$ of the 17 left ventricular segments of the 13 study subjects

and mice (− 139.3 ± 5.8 mV) hearts, with results comparable to those obtained for humans in this study (− 160.7 ± 3.7 mV).

Table 2 Average tissue membrane potential ($\Delta\Psi_T$) for the 17 left ventricular segments

Segments	$\Delta\Psi_T$ (mV)
1	− 160.4 ± 3.7
2	− 159.0 ± 4.3
3	− 161.6 ± 4.1
4	− 163.5 ± 4.0
5	− 161.6 ± 5.2
6	− 161.1 ± 4.4
7	− 160.4 ± 4.5
8	− 159.9 ± 4.2
9	− 162.1 ± 3.9
10	− 164.5 ± 4.0
11	− 163.4 ± 4.9
12	− 162.5 ± 4.5
13	− 161.2 ± 4.4
14	− 158.9 ± 4.2
15	− 161.2 ± 4.7
16	− 162.1 ± 5.2
17	− 154.0 ± 4.4
Left ventricle	− 160.7 ± 3.7

However, the resolution of the PET scanner was very low and quantitation methods are questionable by today's standards. More recently, Gurm et al. reported an attempt to measure myocardial $\Delta\Psi_m$ in vivo with [^{18}F]TPP$^+$ in a swine model of ischemic heart disease [19]. Their results were however discordant with previous in vitro and in vivo studies, with a reported average $\Delta\Psi_m$ of − 91 mV. This is likely related to two critical methodological issues: first, the Nernst equation was applied while tracer concentrations in the blood and myocardium were changing, whereas both the tracer and subject must be in steady state for concentrations to exhibit Nernstian behavior [16, 17]. Second, they did not account for extracellular volume, which would lead to underestimation of $\Delta\Psi_m$. Our group reported the first successful technique to image and quantify $\Delta\Psi_T$ in swine [10]. The $\Delta\Psi_T$ values obtained in that study, which is based on similar methodology, were slightly different (− 129 mV) than those obtained in the present study [10]. We hypothesize that two main factors could explain these differences. First, species variability could account for part of this difference, and second, the use of isoflurane for anesthesia in pigs could lead to partial mitochondrial depolarization [20, 21].

Average $\Delta\Psi_c$ can be estimated from typical ventricular action potential. Assuming a QT of 400 ms, using the average subjects' heart rate of 65 bpm, a polarized (phase 4) $\Delta\Psi_c$ of − 90 mV, and an average depolarized (phase 0–3) $\Delta\Psi_c$ of +

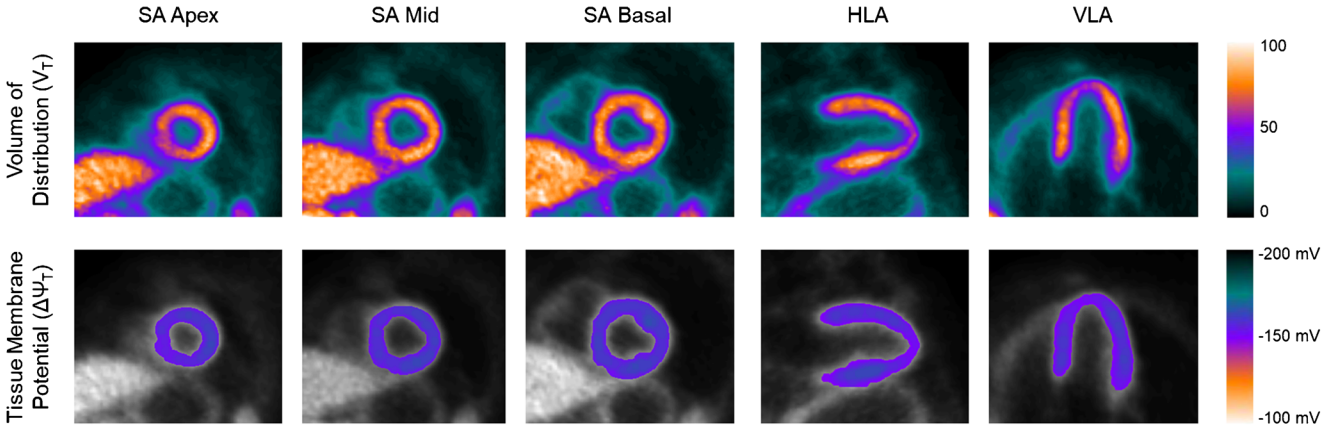

Fig. 2 Parametric image of the volume of distribution (top) and tissue membrane potential (bottom). SA, short axis. HLA, horizontal long axis. VLA, vertical long axis

30 mV (peak + 50 mV), the average $\Delta\Psi_c$ is approximately − 38 mV. Therefore, we can estimate $\Delta\Psi_m$ ($\Delta\Psi_m = \Delta\Psi_T$-$\Delta\Psi_c$) to be − 123 mV. This value is in excellent agreement with the measurements of − 118 mV obtained in explanted intact perfused rat hearts using the Langendorff method and a physiological glucose infusion [9]. It is important to acknowledge that the mitochondrial environment significantly affects $\Delta\Psi_m$, and it must be taken into consideration when comparing in vivo and in vitro measurements. Indeed, it has been shown that in situ assessment of $\Delta\Psi_m$ typically yields smaller values compared to isolated mitochondrion (− 180 to − 190 mV) [22–24]. This can be accounted for by variable substrate availability which alters $\Delta\Psi_m$ [9, 25].

A main limitation of this study is the lack of an in vivo gold standard for the measurement of $\Delta\Psi_m$. However, this technique simply represents the extension of well-established chemistry principles and in vitro methods. Importantly, membrane potential measurements of this study agreed well with those of previous and comparable experiments, supporting the validity of the presented methodology. Another limitation is the fact that the cellular mitochondrial content (f_{mito}) was not quantified and assumed the same for all subjects. However, myocardial mitochondrial morphology and volume is known to be affected in several conditions such as diabetes [26, 27] and heart failure [28]. Unfortunately, in vivo measurement of f_{mito} is not

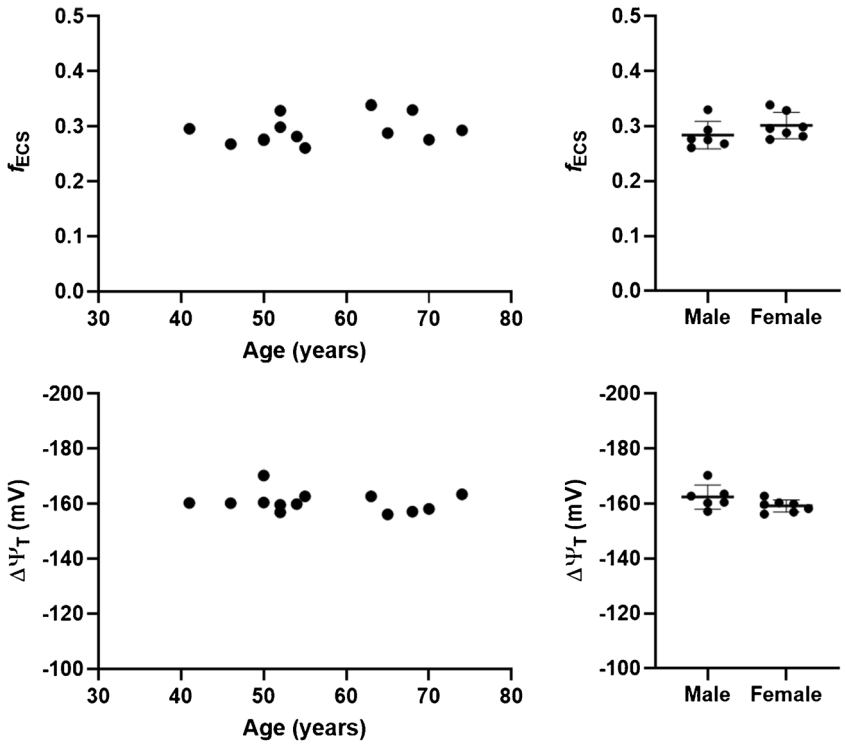

Fig. 3 Extracellular fraction (f_{ECS}) and tissue membrane potential ($\Delta\Psi_T$) versus age (left) and according to sex (right)

currently feasible. Using Eq. 1, we can estimate the variation induced by not accounting for f_{mito}: a change of 10% in f_{mito} will lead to a change of 2–3 mV in $\Delta\Psi_T$. In several pathologies of interest, it is expected that f_{mito} will decrease, leading to overestimation of depolarization (less negative $\Delta\Psi_T$). It should also be noted that f_{mito} enters Eq. 1 as constant multiplier, meaning that for normal human subjects, systematic errors in f_{mito} do not affect the method's ability to compare subjects or groups. Another limitation of this study is its small sample size. Nonetheless, this study demonstrated the feasibility of in vivo measurements of membrane potential in humans. Finally, 2 subjects had a medical history of hypertension and 3 subjects had a systolic blood pressure > 130 mmHg at time of imaging, which could affect the measured $\Delta\Psi_T$.

Conclusion

We demonstrated for the first time the feasibility of non-invasive, in vivo, quantitative assessment of cardiac $\Delta\Psi_T$ in humans, with very low variability of $\Delta\Psi_T$ between subjects meaning that relatively small sample size would be sufficient for hypotheses testing. Furthermore, true quantitation provided by this method allows comparison between subjects and enables the investigation of several pathologies of interest such as diabetes and chemotherapy-induced cardiotoxicity, which are typically associated with diffuse myocardial involvement. $\Delta\Psi_T$ has the potential to provide early diagnosis for various pathologies, including cardiotoxicity. In addition, given the new therapies targeting the mitochondria, $\Delta\Psi_T$ could serve as a surrogate endpoint in clinical trials and be used for the assessment of response to therapy. Finally, the method is generalizable to other organs and tissue and could be used for characterization of tumors [29]. More studies are required to assess these potential roles.

Funding information This study was funded by the NIH (grant numbers: P41EB022544 R01HL137230 T32EB013180).

Compliance with ethical standards

Disclosures None.

Conflict of interest The authors declare that they have no conflict of interest.

Ethical approval All procedures performed in studies involving human participants were in accordance with the ethical standards of the institutional and/or national research committee (The Partners Human Research Committee) and with the 1964 Helsinki declaration and its later amendments or comparable ethical standards.

Informed consent Informed consent was obtained from all individual participants included in the study.

References

1. Lin L, Sharma VK, Sheu S-S. Mechanisms of reduced mitochondrial Ca2+ accumulation in failing hamster heart. Pflugers Arch - Eur J Physiol. 2007;454:395–402.
2. Rasola A, Bernardi P. Mitochondrial permeability transition in Ca(2+)-dependent apoptosis and necrosis. Cell Calcium. 2011;50:222–33.
3. Rutledge C, Dudley S. Mitochondria and arrhythmias. Expert Rev Cardiovasc Ther. 2013;11:799–801.
4. Turer AT, Hill JA. Pathogenesis of myocardial ischemia-reperfusion injury and rationale for therapy. Am J Cardiol. 2010;106:360–8.
5. O'Rourke B, Cortassa S, Aon MA. Mitochondrial ion channels: gatekeepers of life and death. Physiology (Bethesda). 2005;20:303–15.
6. Hüttemann M, Lee I, Pecinova A, Pecina P, Przyklenk K, Doan JW. Regulation of oxidative phosphorylation, the mitochondrial membrane potential, and their role in human disease. J Bioenerg Biomembr. 2008;40:445–56.
7. Kauppinen R. Proton electrochemical potential of the inner mitochondrial membrane in isolated perfused rat hearts, as measured by exogenous probes. Biochim Biophys Acta. 1983;725:131–7.
8. Rottenberg H. Membrane potential and surface potential in mitochondria: uptake and binding of lipophilic cations. J Membr Biol. 1984;81:127–38.
9. Wan B, Doumen C, Duszynski J, Salama G, Vary TC, LaNoue KF. Effects of cardiac work on electrical potential gradient across mitochondrial membrane in perfused rat hearts. Am J Phys. 1993;265:H453–60.
10. Alpert NM, Guehl N, Ptaszek L, Pelletier-Galarneau M, Ruskin J, Mansour MC, et al. Quantitative in vivo mapping of myocardial mitochondrial membrane potential. PLoS One. 2018;13:e0190968.
11. Barth E, Stämmler G, Speiser B, Schaper J. Ultrastructural quantitation of mitochondria and myofilaments in cardiac muscle from 10 different animal species including man. J Mol Cell Cardiol. 1992;24:669–81.
12. Elmaleh D, Kardan A, Barrow S, Dragotakes S, Correia J, Weise S, et al. A phase I study evaluating dosimetry and myocardial pharmacokinetic behavior of BFPET, a new F-18 labeled tracer for myocardial perfusion imaging. J Nucl Med. Society of Nuclear Medicine; 2009;50:420–420.
13. Messroghli DR, Radjenovic A, Kozerke S, Higgins DM, Sivananthan MU, Ridgway JP. Modified look-locker inversion recovery (MOLLI) for high-resolution T1 mapping of the heart. Magn Reson Med. 2004;52:141–6.
14. Paulus DH, Quick HH, Geppert C, Fenchel M, Zhan Y, Hermosillo G, et al. Whole-body PET/MR imaging: quantitative evaluation of a novel model-based MR attenuation correction method including bone. J Nucl Med. 2015;56:1061–6.
15. Fukuda H, Syrota A, Charbonneau P, Vallois J, Crouzel M, Prenant C, et al. Use of 11C-triphenylmethylphosphonium for the evaluation of membrane potential in the heart by positron-emission tomography. Eur J Nucl Med. 1986;11:478–83.
16. Dedkova EN, Blatter LA. Measuring mitochondrial function in intact cardiac myocytes. J Mol Cell Cardiol. 2012;52:48–61.
17. Duchen MR, Surin A, Jacobson J. Imaging mitochondrial function in intact cells. Meth Enzymol. 2003;361:353–89.
18. McCluskey S, Haslop A, Coello C, Gunn R, Tate E, Southworth R, et al. Imaging chemotherapy induced acute cardiotoxicity with 18F-labelled lipophilic cations. J Nucl Med. 2019.
19. Gurm GS, Danik SB, Shoup TM, Weise S, Takahashi K, Laferrier S, et al. 4-[18F]-Tetraphenylphosphonium as a PET tracer for myocardial mitochondrial membrane potential. JACC Cardiovasc Imaging. 2012;5:285–92.

20. Zhang Y, Dong Y, Wu X, Lu Y, Xu Z, Knapp A, et al. The mitochondrial pathway of anesthetic Isoflurane-induced apoptosis. J Biol Chem. 2010;285:4025–37.
21. Loop T, Dovi-Akue D, Frick M, Roesslein M, Egger L, Humar M, et al. Volatile anesthetics induce caspase-dependent, mitochondria-mediated apoptosis in human T lymphocytes in vitro. Anesthesiology. 2005;102:1147–57.
22. Gerencser AA, Chinopoulos C, Birket MJ, Jastroch M, Vitelli C, Nicholls DG, et al. Quantitative measurement of mitochondrial membrane potential in cultured cells: calcium-induced de- and hyperpolarization of neuronal mitochondria. J Physiol. 2012;590:2845–71.
23. Kamo N, Muratsugu M, Hongoh R, Kobatake Y. Membrane potential of mitochondria measured with an electrode sensitive to tetraphenyl phosphonium and relationship between proton electrochemical potential and phosphorylation potential in steady state. J Membr Biol. 1979;49:105–21.
24. Hafner RP, Brown GC, Brand MD. Analysis of the control of respiration rate, phosphorylation rate, proton leak rate and protonmotive force in isolated mitochondria using the "top-down" approach of metabolic control theory. Eur J Biochem. 1990;188:313–9.
25. Ainscow EK, Brand MD. Internal regulation of ATP turnover, glycolysis and oxidative phosphorylation in rat hepatocytes. Eur J Biochem. 1999;266:737–49.
26. Makino A, Suarez J, Gawlowski T, Han W, Wang H, Scott BT, et al. Regulation of mitochondrial morphology and function by O-GlcNAcylation in neonatal cardiac myocytes. Am J Physiol Regul Integr Comp Physiol. 2011;300:R1296–302.
27. Yu T, Sheu S-S, Robotham JL, Yoon Y. Mitochondrial fission mediates high glucose-induced cell death through elevated production of reactive oxygen species. Cardiovasc Res. 2008;79:341–51.
28. Gupta A, Gupta S, Young D, Das B, McMahon J, Sen S. Impairment of ultrastructure and cytoskeleton during progression of cardiac hypertrophy to heart failure. Lab Investig. 2010;90:520–30.
29. Momcilovic M, Jones A, Bailey ST, Waldmann CM, Li R, Lee JT, et al. In vivo imaging of mitochondrial membrane potential in non-small-cell lung cancer. Nature. 2019;575:380–4.